



Sharp Alfvénic Impulses in the Near-Sun Solar Wind

Timothy Horbury, Thomas Woolley, Ronan Laker, Lorenzo Matteini, Jonathan Eastwood, Stuart Bale, Marco Velli, Benjamin Chandran, Tai Phan, Nour Raouafi, et al.

► To cite this version:

Timothy Horbury, Thomas Woolley, Ronan Laker, Lorenzo Matteini, Jonathan Eastwood, et al.. Sharp Alfvénic Impulses in the Near-Sun Solar Wind. The Astrophysical Journal Supplement, 2020, 246 (2), pp.45. 10.3847/1538-4365/ab5b15 . insu-02937595

HAL Id: insu-02937595

<https://insu.hal.science/insu-02937595>

Submitted on 18 Sep 2020

HAL is a multi-disciplinary open access archive for the deposit and dissemination of scientific research documents, whether they are published or not. The documents may come from teaching and research institutions in France or abroad, or from public or private research centers.

L'archive ouverte pluridisciplinaire **HAL**, est destinée au dépôt et à la diffusion de documents scientifiques de niveau recherche, publiés ou non, émanant des établissements d'enseignement et de recherche français ou étrangers, des laboratoires publics ou privés.

Sharp Alfvénic impulses in the near-Sun solar wind

TIMOTHY S. HORBURY,¹ THOMAS WOOLLEY,¹ RONAN LAKER,¹ LORENZO MATTEINI,¹ JONATHAN EASTWOOD,¹
STUART D. BALE,^{2,3} MARCO VELLI,⁴ BENJAMIN D. G. CHANDRAN,^{5,6} TAI PHAN,³ NOUR E. RAOUAFI,⁷ KEITH GOETZ,⁸
PETER R. HARVEY,³ MARC PULUPA,⁹ K.G. KLEIN,¹⁰ THIERRY DUDOK DE WIT,¹¹ JUSTIN C. KASPER,^{12,13}
KELLY E. KORRECK,¹³ A. W. CASE,¹³ MICHAEL L. STEVENS,¹³ PHYLLIS WHITTLESEY,⁹ DAVIN LARSON,⁹
ROBERT J. MACDOWALL,¹⁴ DAVID M. MALASPINA,¹⁵ AND ROBERTO LIVI⁹

¹*Imperial College London, South Kensington Campus, London SW7 2AZ, UK*

²*Physics Department, University of California, Berkeley, CA 94720-7300, USA*

³*Space Sciences Laboratory, University of California, Berkeley, CA 94720-7450, USA*

⁴*Institute of Geophysics and Planetary Physics (IGPP), Department of Earth, Planetary and Space Sciences (EPSS) University of California, Los Angeles*

⁵*Department of Physics & Astronomy, University of New Hampshire, Durham, NH 03824, USA*

⁶*Space Science Center, University of New Hampshire, Durham, NH 03824, USA*

⁷*Johns Hopkins University Applied Physics Laboratory, 11100 Johns Hopkins Road, Laurel, Maryland 20723-6099, USA*

⁸*School of Physics and Astronomy, University of Minnesota, Minneapolis, MN 55455, USA*

⁹*University of California, Berkeley, CA, USA*

¹⁰*Lunar and Planetary Laboratory, University of Arizona, Tucson, AZ 85719, USA.*

¹¹*LPC2E, CNRS and University of Orléans, Orléans, France*

¹²*University of Michigan, Ann Arbor, MI, USA*

¹³*Smithsonian Astrophysical Observatory, Cambridge, MA, USA*

¹⁴*Solar System Exploration Division, NASA/Goddard Space Flight Center, Greenbelt, MD, 20771*

¹⁵*Laboratory for Atmospheric and Space Physics, University of Colorado, Boulder, CO 80303, USA*

(Received October 3, 2019; Revised some date; Accepted November 20, 2019)

Submitted to AJ

ABSTRACT

Measurements of the near-Sun solar wind by Parker Solar Probe have revealed the presence of large numbers of discrete Alfvénic impulses with an anti-Sunward sense of propagation. These are similar to those previously observed near 1 AU, in high speed streams over the Sun’s poles and at 60 solar radii. At 35 solar radii, however, they are typically shorter and sharper than seen elsewhere. In addition, these spikes occur in “patches” and there are also clear periods within the same stream when they do not occur; the timescale of these patches might be related to the rate at which the spacecraft magnetic footpoint tracks across the coronal hole from which the plasma originated. While the velocity fluctuations associated with these spikes are typically under 100 km/s, due to the rather low Alfvén speeds in the streams observed by the spacecraft to date, these are still associated with large angular deflections of the magnetic field - and these deflections are not isotropic. These deflections do not appear to be related to the recently reported large scale, pro-rotation solar wind flow. Estimates of the size and shape of the spikes reveal high aspect ratio flow-aligned structures with a transverse scale of $\approx 10^4$ km. These events might be signatures of near-Sun impulsive reconnection events.

Keywords: solar wind, corona, plasmas

1. INTRODUCTION

Early measurements of the solar wind near the Earth revealed the presence of coherent streams, lasting several days, of relatively high speed (> 500 km/s) plasma with a single polarity. These fast streams originate in regions of open magnetic field in the Sun’s corona, known as coronal holes (e.g. [Cranmer 2002](#)). In contrast to slower, more variable wind, coronal hole streams are rather homogeneous on scales of minutes to hours and are pervaded by large amplitude magnetohydrodynamic fluctuations which are Alfvénic in nature and have an anti-Sunward sense of propagation in the plasma frame ([Bruno & Carbone 2013](#)).

The fundamental thermodynamics of the generation of the solar wind from a region of open magnetic field are relatively well understood ([Cranmer 2002](#)), but it is clear that the fastest wind cannot be generated from a corona of the observed temperatures without an additional driving mechanism, such as waves or impulsive reconnection-driven events. While signatures of both waves and nano-flares are observed remotely in the solar atmosphere, the pervasive Alfvénic fluctuations measured in situ in the solar wind have often been interpreted as being the remnants of coronal waves and indeed their contribution to the solar wind energy and momentum budget has been assessed ([De Pontieu et al. 2007](#)).

Coronal transients (jets, spicules, etc.) are near-ubiquitous phenomena that are observed all over the solar disk and throughout the solar activity cycle. Coronal jets (see [Raouafi et al. 2016](#), for a recent comprehensive review) are, as seen in X-ray and EUV images, impulsive, beam-like structures ([Cirtain et al. 2007](#)). Remote observations of coronal jets reveal a diverse range of phenomena over a broad range of scales. As successive improvements have been made in the spatial and temporal resolution of remote observations, along with increased sensitivity, jet-like structures have been revealed on successively smaller scales. We do not attempt a review of this field, but note a few key observational characteristics: at least some jets last tens of seconds and are very narrow (≈ 300 km; [Tian et al. 2014](#)) but elongated along the local magnetic field, propagating at a few hundred km/s, near the local Alfvén speed. Many originate in coronal holes; they are often associated with transverse magnetic field motion, which is sometimes helical ([Patsourakos et al. 2008](#)). The plasma associated with jets does not always escape into deep space and its ultimate trajectory is determined by the magnetic field orientation above the jet ([Culhane et al. 2007](#)). Jets can be associated with the longer lived, and more diverse, plumes that can be observed above coronal holes ([Raouafi et al. 2008](#)). The ultimate cause of jets is not entirely clear, but magnetic reconnection seems likely to play a key role.

[Raouafi & Stenborg \(2014\)](#) discovered a new phenomenon of high magnetic activity at small scales. Using high resolution EUV images and magnetograms from the Solar Dynamic Observatory, they observed small and short lived transients occurring at the footpoints of plumes with coronal holes. They called these transients jetlets and it is believed that the jetlet results from magnetic reconnection similar to nominal jets. The only difference is the frequency of this new phenomenon. Jetlets are naturally short-lived with lifetimes ranging from few tens of seconds to a few minutes.

Jets are also seen off-limb out to several solar radii (e.g., [Wang et al. 1998](#); [Yu et al. 2014](#); [Dobrzycka et al. 2002](#)) although a difference in plasma properties, typically density, relative to the background is required for such identification. The interplanetary signatures of coronal transients such as nano-flares, spicules and jets are not clear, although there is some evidence for an association between solar wind speed enhancements on the scale of hours known as “microstreams,” and polar plumes ([Neugebauer 2012](#)). Recent simulations of coronal jets ([Uritsky et al. 2017](#); [Wyper et al. 2017](#)) show Alfvénic fluctuations propagating to high altitudes. [Roberts et al. \(2018\)](#) simulated jets out to 35 solar radii (R_S) and showed that observable signatures in the plasma speed and magnetic field could be present but without significant density variations. While the jets simulated by [Roberts et al. \(2018\)](#) were much larger than the events considered here, nevertheless the qualitative predictions are of interest: they suggest that an originally discrete and coherent jet will, as it propagates, generate considerable substructure so that at tens of solar radii, while the overall form of an elongated structure remains, the signature at a spacecraft could be very complex. Recently, simulations by [Tenerani \(2019\)](#) have shown that Alfvénic structures such as those that could be produced by jets can indeed survive in the solar wind out to tens of solar radii.

By the time it arrives near the Earth, the solar wind has spent several days in transit from the outer corona, during which time the fluctuations evolve dynamically and interactions between parcels with different speeds and pressures can mask the original state of the plasma. Measurements of the solar wind closer to the Sun are therefore of considerable interest in determining the original dynamical state of the wind. Data from the twin Helios spacecraft near perihelion at 0.3 AU ($\approx 60 R_S$) showed a qualitatively similar picture to that at 1 AU, although since $\delta\mathbf{B}/|B| \approx 1$ at both distances, with an Alfvén speed of ≈ 150 km/s the resulting velocity fluctuations were considerably higher amplitude at Helios than at larger distances.

The anti-Sunward sense of propagation of the fluctuations in coronal hole streams results in an asymmetry in the resulting velocity variations, with a preference for enhancements in the speed, at least when the background magnetic field direction is close to radial, or equivalently the Parker spiral angle $\phi_P = \tan^{-1}(B_T/B_R)$ is relatively small: $\phi_P \approx 45^\circ$ at 1 AU and $\phi_P \approx 10^\circ$ at 0.3 AU. Here we use the RTN coordinate system (Hapgood 1992) where R points anti-sunward, T is the cross product of R with the solar rotation vector and N completes the right-handed set. The tendency for speed enhancements was first identified in near-Earth data by Gosling et al. (2011) and explained in more detail by Matteini et al. (2014) using high latitude high speed wind measurements. Horbury et al. (2018) showed that at 0.3 AU, these speed enhancements were large and, crucially, appeared to be isolated and intermittent rather than a homogeneous population of waves. They suggested that these structures might be the interplanetary signatures of coronal reconnection-driven jets, and hence that the solar wind might be driven, in part, by these jets rather than just waves.

Launched in August 2018, Parker Solar Probe (PSP; Fox et al. 2016) has now sampled the solar wind far closer than before, with a perihelion of just $35 R_S$. During its first perihelion, PSP encountered slow wind from a small equatorial coronal hole and revealed the presence of isolated intermittent velocity enhancements associated with magnetic field deflections, which have many similarities with those seen in earlier observations, but with some important differences (Bale 2019; Kasper 2019). In this paper, we use magnetic field measurements from the FIELDS instrument (Bale et al. 2016) and bulk plasma measurements from the SWEAP instrument (Kasper et al. 2016), present some of these events and describe some of their key properties, including their durations and amplitudes. We demonstrate that their orientations are not randomly distributed and make the first estimate of the size and shape of the structures, showing that they are likely to be high aspect ratio structures with their long axis aligned with the flow. We compare measurements from two solar wind streams at different distances and show that these are consistent with similar structures being present in both. Finally, we discuss the potential link between these structures and transient coronal events, particularly coronal jets.

We note in passing that there is as yet no consensus on a name for the isolated structures discussed here. The large magnetic field deflections, which can exceed 90° , have led some to term them “switchbacks” (Bale 2019; Dudok de Wit et al. 2019), while the enhanced plasma speed has led to them being termed “jets” (Kasper 2019). Here, we avoid either of these terms, particularly because the latter could cause confusion with remotely-observed coronal jets whose causal link to these events is not fully established. Following Horbury et al. (2018), we therefore use the more neutral term “spikes” to describe the observational signatures.

2. SPIKES AT 35 SOLAR RADII

Many spikes are visible in Figure 1, most easily as sharp variations in B_R , many of which cause the radial component to change sign. These are not changes in magnetic polarity (Kasper 2019; Whittlesey 2019), but reversals in the field. They are associated with increases in V_R and are largely Alfvénic, with highly correlated variations in all three components of B and V .

One striking aspect of the spikes in Figure 1 is that they occur in “patches” lasting several hours separated by times when the magnetic field is very quiet and close to the Parker spiral direction; during these quiet times the radial proton bulk speed V_R is rather lower than elsewhere. While the quiet regions are not entirely free from spikes, the difference is clear; Bale (2019) have recently reported that these quiet periods, with nearly radial field, support a distinct population of kinetic waves. While there is necessarily a qualitative aspect to identifying patch and non-patch regions, patches seem to fill at least three quarters of the time near perihelion.

A shorter period of data is shown in Figure 2 where individual spikes can be seen as variations in B_R away from the background Parker spiral value: since ϕ_P is small, this is approximately the field magnitude. A patch of spikes ends at approximately 17:15 in Figure 2, when the overall fluctuation level decreases, although there are still spikes after this time. We note some other typical, but not ubiquitous, features of spikes: $|B|$ is often smaller on average in patches than outside (Bale 2019) and there are some significant short decreases in the field in some spikes. The duration of spikes varies widely, with some lasting over ten minutes but some lasting only seconds. Some have sharp boundaries, while others show rather slower variations in B_R . In general, the magnetic field direction returns to its original orientation following a spike – that is, there is no evidence that spikes are, overall, current sheets separating two separate magnetic topologies, as might be expected across a simple reconnection jet outflow (Phan 2019).

We stress that not all MHD-scale fluctuations during perihelion are what we might term spikes. Isolated wave-like structures are present at times, along with small scale fluctuations. Here, though, we concentrate on the spikes which

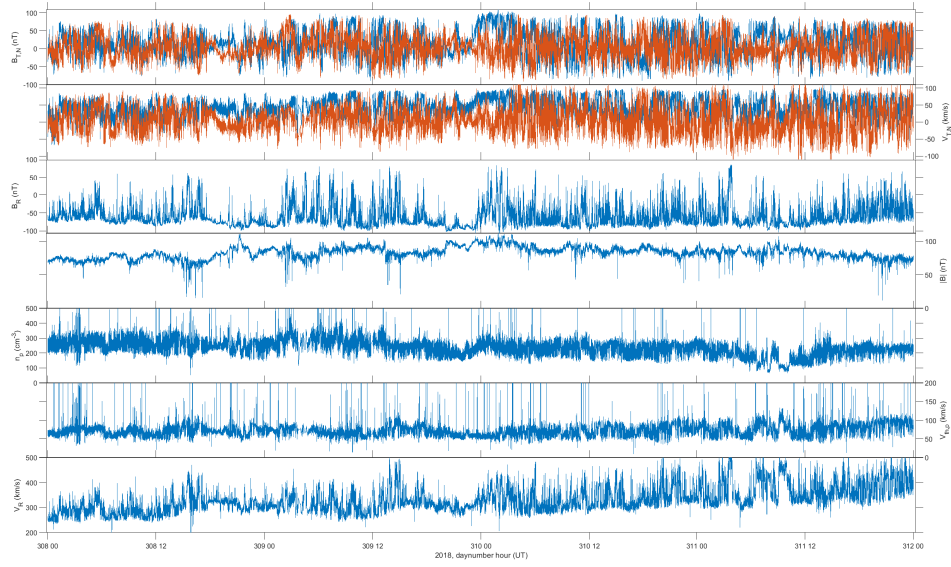


Figure 1. Two days around perihelion for encounter 1. Panels show from top to bottom: T (blue) and N (red) components of the magnetic field; T (blue) and N (red) components of the proton bulk velocity; R (radial) component of the magnetic field; magnetic field magnitude; proton core density; proton core thermal speed; and proton core radial speed. Spikes are visible as increases in B_R and V_R . The high correlation between magnetic field and velocity fluctuations demonstrates their largely Alfvénic nature.

appear to be the dominant fluctuation power on MHD scales; the relation of these to the local turbulent cascade is discussed by [Dudok de Wit et al. \(2019\)](#).

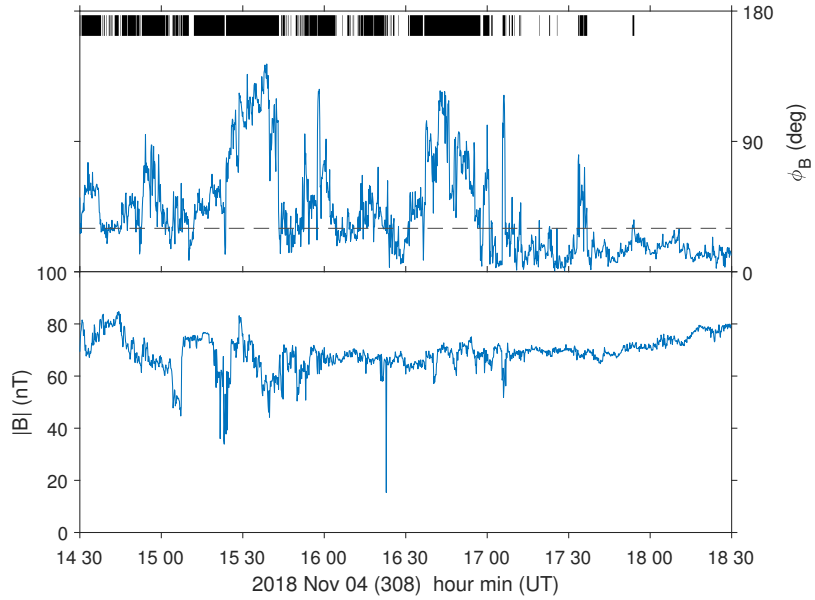


Figure 2. A series of spikes. Panels are the angle of the magnetic field from the Parker spiral and magnitude of the magnetic field respectively. Spikes identified by the algorithm described in section 2.1 are identified by thick bars in the top panel; the threshold angle is shown as a dashed line.

The events described here are, in many ways, similar to those previously observed, particularly those at $60 R_S$ by Helios (Horbury et al. 2018). They are short (seconds to minutes) Alfvénic deflections in the magnetic field and velocity, resulting in velocity enhancements. They are very common, but there are times when they are not present, when the wind is typically slower and fluctuations are generally much lower (c.f. Figure 8 of Horbury et al. 2018). Nevertheless, there are some differences, perhaps the most striking being the much lower amplitudes of the velocity enhancements compared to those at Helios, where the bulk velocity could reach 1000 km/s. This is due both to the background wind speed being low and Alfvén speed being small: since the maximum speed enhancement is twice the Alfvén speed (Matteini et al. 2014) this means that the actual velocity spikes were rather modest.

The grouping of spikes into patches is not clear in Helios data, although what we might term the “filling factor,” the fraction of the time when spikes were generally present, seems at least roughly comparable at around three quarters of the stream – this is a remarkably high fraction and suggests that spikes must play a significant role in the dynamics of wind from coronal holes.

2.1. Automated identification of spikes

While spikes are often clear by eye in the time series, in order to study them in a more systematic manner, they were identified using an algorithm similar to that used by Horbury et al. (2018). A spike was considered to start when the magnetic field vector (using 1 vector/s data) deflected more than 30° from the local Parker spiral direction (based on the spacecraft solar distance and background solar wind speed), and end when it returned below this value. Other thresholds (45° , 90°) were used but our results are not very sensitive to this value other than identifying fewer spikes when using a larger threshold. Spikes with durations less than 5s were rejected; again, the results are not very sensitive to this value. In the four day period (4-7 November 2018) around perihelion, 2206 spikes were identified, with a mean duration of 73 s and a mode of 9 s; they covered 46% of the interval. Bars on the top panel of Figure 2 show the spikes identified during this time.

While it is clear from Figure 1 that fluctuations associated with spikes are large and are present in all components of the magnetic field, these are not entirely random. Indeed, although not shown explicitly here, in general the magnetic field vectors within a spike lie along a single arc (great circle), rather than having a helical structure. For each spike, the mean magnetic field vector within it was calculated and its direction with respect to the local Parker spiral angle was determined, as the angle of the vector projected on to the plane perpendicular to the Parker direction that also contains the N direction. This is the TN plane rotated so that it is perpendicular not to R, but the Parker spiral direction. Effectively, this procedure finds the component of the field deflection that is perpendicular to the Parker spiral. For this perpendicular vector, its direction in this plane was characterised by its “clock angle” where $0, 90, 180, 270^\circ$ correspond respectively to the +N, +T, -N, -T directions. Since the Parker spiral angle during perihelion was between 10 and 15° from the radial, this rotation into the Parker direction has only a small effect on the results presented here.

The clock angles of the spike magnetic field deflections are shown in the top panel of Figure 3 as circles, whose area is proportional to their duration. Despite a very broad distribution, nearby spikes tend to have similar clock angles. In part this could be due to the identification of multiple spikes from the same physical event due to fluctuations in the field vector around the 30° criterion angle, but the consistency in deflection direction can last several hours, longer than any realistic single event. There is also some evidence for progressive changes in orientation over a few hours within a patch and a clear tendency for longer duration (larger circles) spikes to have deflections with clock angles near 90° , which corresponds approximately to the +T direction.

During its first encounter, PSP measured a persistent, significant transverse deflection in the mean flow close to the Sun (Kasper 2019) which reached around 30 km/s in the +T direction at perihelion. Since long duration spikes often deflect in this direction, one might therefore conclude that the spikes cause this deflection in the mean flow speed and that in the absence of spikes, there would be no mean flow deflection. However, this does not seem to be the case. In order to demonstrate this, we need to identify the background flow direction in the absence of the spikes.

2.2. Identifying the underlying plasma frame

The deHoffman Teller (HT) frame in a plasma (e.g. Khrabrov & Sonnerup 1998) is one where the electric field is zero. It is widely used in shock analysis but can be applied elsewhere. In particular, while it can be calculated at any individual point in space using electric and magnetic field measurements, it can also be determined in a statistical sense over an interval using magnetic field and velocity data. This procedure identifies a frame where the magnetic field structure is stationary: in general, such a frame need not exist over a finite volume in a plasma, but if the plasma is dominated by Alfvénic fluctuations of one sense of propagation, in essence it identifies their propagation velocity.

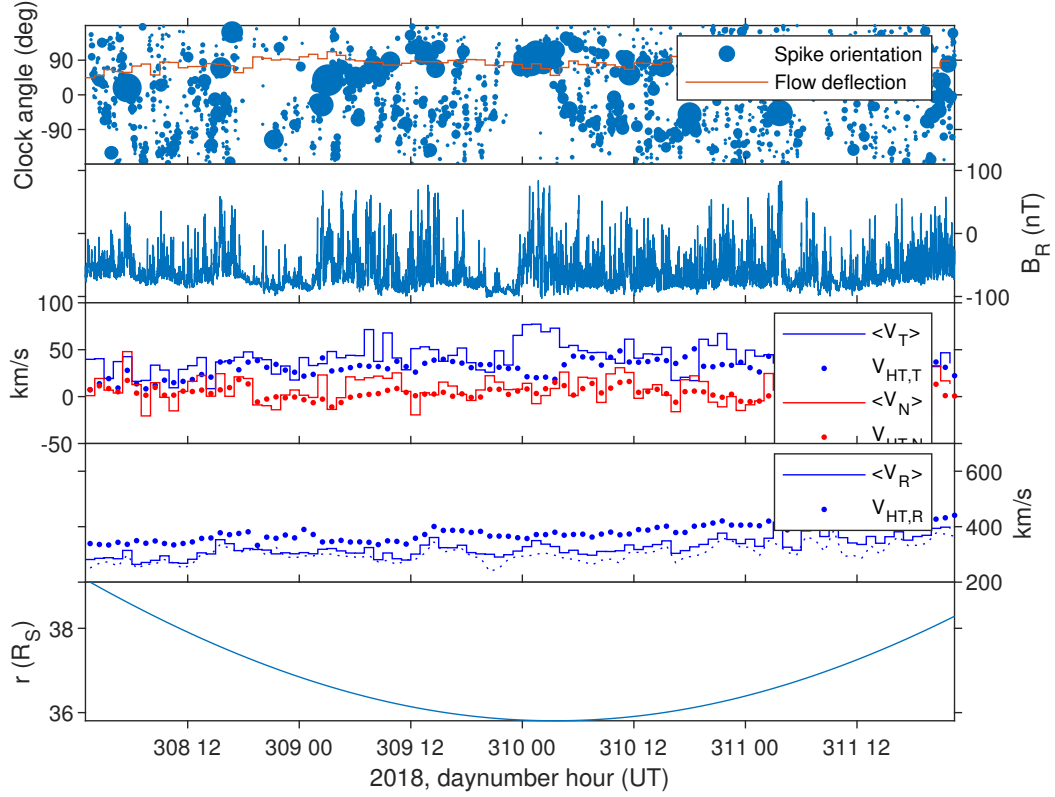


Figure 3. Panels from top: clock angle in the TN plane of the background \mathbf{V}_{HT} (solid line) and the mean magnetic field in spikes (dots: size corresponds to duration); radial field component; T and N components of the mean proton solar wind speed (stepped line) and \mathbf{V}_{HT} (dots); same for the R component; solar distance.

The procedure of identifying the de Hoffman Teller frame \mathbf{V}_{HT} is straightforward (Khrabrov & Sonnerup 1998) and uses a period of magnetic field $\mathbf{B}(t)$ and velocity vectors $\mathbf{V}(t)$ (we use one hour intervals here) to find \mathbf{V}_{HT} by minimising the quantity

$$\sum_t |[\mathbf{V}(t) \times \mathbf{B}(t)] - [\mathbf{V}_{HT} \times \mathbf{B}(t)]| \quad (1)$$

in a least squares sense. In the presence of outward-propagating Alfvénic fluctuations this procedure is remarkably robust. In this frame, Alfvénic velocity fluctuations are located on a sphere centred at zero with a radius of the Alfvén speed V_A : a simple test of the success of this procedure is then to compare the angles of magnetic field vectors with those of the velocity in this frame, where the agreement is normally very good.

To our knowledge the HT frame has not previously been applied to large scale solar wind data and we will return in a later work to a more detailed discussion of its properties, which are of interest in identifying large scale stream structure: it is also related to the frame in which heavy ions such as alphas stream during Alfvénic periods (e.g. Matteini et al. 2015). The invariance of the latter frame in the presence of such fluctuations was previously noted in Helios data by Thieme et al. (1990). The HT frame is neither the mean solar wind velocity $\langle \mathbf{V}_P \rangle$, or the bulk velocity in the absence of any Alfvénic fluctuations \mathbf{V}_0 ; here, we calculate boxcar means over one hour periods. The components of $\langle \mathbf{V}_P \rangle$ and \mathbf{V}_{HT} are compared in Figure 3, where significant differences can be seen. In principle, \mathbf{V}_{HT} lies a distance V_A in velocity space away from \mathbf{V}_0 along the Parker spiral direction and in practice the radial component of \mathbf{V}_{HT} is larger than that of $\langle \mathbf{V}_P \rangle$ by around the local Alfvén speed, which here is around 60 km/s while $\langle V_0 \rangle \approx 350$ km/s, as can be seen in panel 4 of Figure 3. While we could subtract V_A along the Parker spiral direction to achieve our best estimate of \mathbf{V}_0 , we have chosen here to simply use \mathbf{V}_{HT} as our estimate of the underlying plasma flow direction, since it is approximately co-aligned with \mathbf{V}_0 .

The utility of \mathbf{V}_{HT} is that it identifies a frame which does not vary in the presence of any individual Alfvénic fluctuation such as a spike and we can therefore use it to quantify any underlying flow deflections, which would otherwise not be possible since the asymmetry of spike velocity deflections would bias the calculation of a mean velocity. Figure 3 shows significant differences between \mathbf{V}_{HT} and the mean velocity, with the former generally being more stable, while the latter is greatly affected by spikes. The systematic value of ≈ 30 km/s in the +T direction is the flow deflection identified by Kasper (2019) and we can see that there is no similar deflection in the N direction. The clock angle of \mathbf{V}_{HT} is shown on the top panel of Figure 3 where its consistent value around $+90^\circ$, corresponding to a deflection in +T, is clear. Crucially, this does not vary, even while the spike deflection changes between patches. This is strong evidence that the flow deflection is not caused by spikes. Indeed, while during this interval the flow is consistently deflected in +T, as shown in Figure 4, the spikes are not. Rather, they show a tendency to deflect in both +T and -T rather than other directions. This is a weak result, but seems to be present in other intervals of data in perihelia 1 and 2.

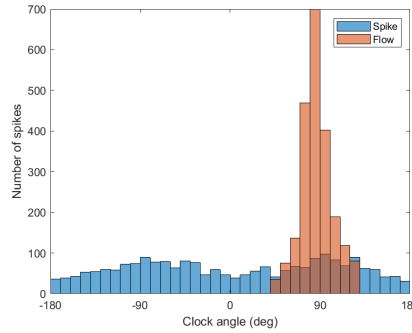


Figure 4. Histogram of the clock angle in the TN plane, of (red) the background flow velocity V_{HT} and (blue) the mean magnetic field deflection in a spike.

3. SIZE AND SHAPE

The spikes within the perihelion stream of encounter 1 have a wide range of durations at the spacecraft. Whatever the physical origin of these structures, it is inevitable that they exist over a range of scales (Dudok de Wit et al. 2019). Nevertheless, it is possible to use the information on the distribution of durations to infer additional information about the properties of the spikes.

There is a correlation between the duration of spikes and the mean magnetic field deflection within them (Figure 5). This could have many causes: any structure that has a finite size, with a larger field deflection nearer its centre than its edge, will inevitably produce such a correlation depending on how deep the spacecraft cuts through it. Of more interest is a correlation between the duration of the spikes at the spacecraft and the transverse velocity of the spacecraft through them. This is shown in Figure 6 and merits a detailed discussion.

3.1. Determining spike shape using flow deflections

The instantaneous velocity of the plasma relative to the spacecraft $\mathbf{V}_{Rel} = \mathbf{V}_P - \mathbf{V}_{SC}$, where \mathbf{V}_{SC} is the spacecraft velocity, is shown schematically in Figure 7. The perihelion stream in encounter 1 was unusually slow for a coronal hole flow, with background speeds $\mathbf{V}_P \approx 300 - 500$ km/s. The ≈ 30 km/s transverse, +T, component resulted in the wind propagating on average at an angle of around 6° from radial, an unusually large deflection. The spacecraft itself was travelling at $V_{SC} \approx 90$ km/s in approximately the +T direction as a result of its eccentric orbital motion and hence relative to the spacecraft, the background wind was travelling in the -T direction as well as in +R, since the spacecraft speed in +T was greater than the flow deflection speed.

Alfvénic velocity fluctuations due to spikes moved the velocity V_P around the sphere centred on V_{HT} . When this deflection was towards -T (panel (c) of Figure 7), this resulted in V_{Rel} being at large angles to the radial, up to 20° - a far larger angle of the sampling direction to the radial than has ever been experienced by a spacecraft before. In contrast, a spike with a deflection of V_P towards +T (panel (d)) would result in V_R being near radial. There is therefore a systematic dependence on the direction through which the spikes were sampled, and the direction of the velocity

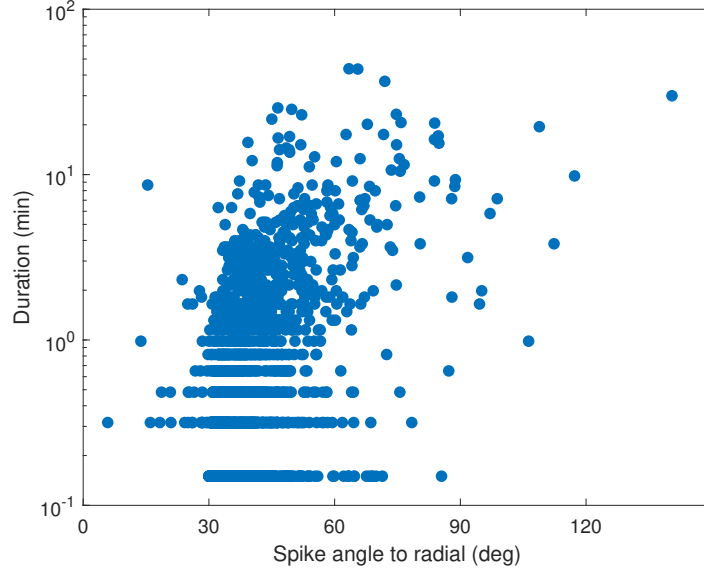


Figure 5. Duration of spikes at the spacecraft as a function of the mean field deflection within them. While there is a lot of scatter, longer spikes tend to have larger angular deflections on average.

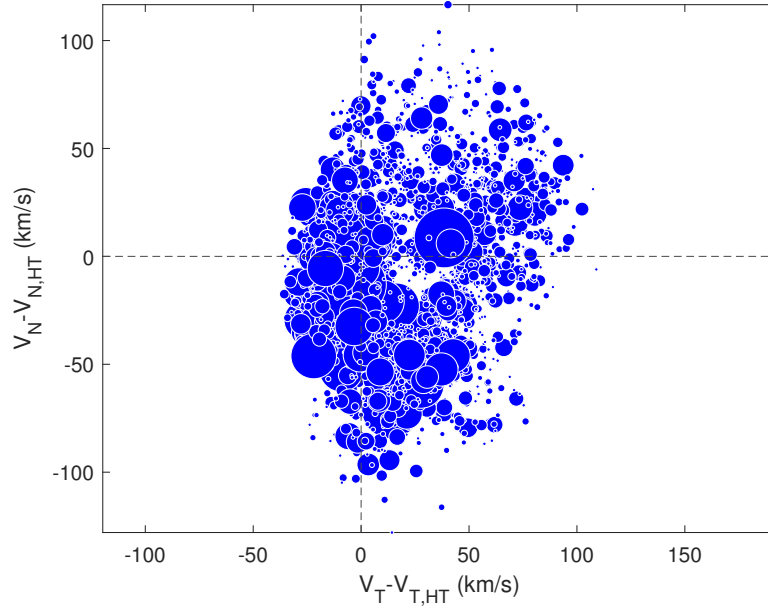


Figure 6. Mean velocity within each spike, in the (T,N) plane, relative to the local deHoffman Teller frame. The dot area is proportional to the duration of each spike. While the variation is large, spikes tend to be longer in duration when the transverse velocity is nearer zero.

and field deflection within them. It appears that this might be responsible for the dependence of spike duration on transverse velocity seen in Figure 6.

If the spike structures are fundamentally long and thin, aligned approximately radially, then depending on the angle at which the spacecraft passed through them, one would expect their spatial extent to vary: passing through the long axis of a cigar-like structure would naturally result in a longer extent than crossing perpendicular to it. This is consistent with Figure 6 where the longer duration (and hence spatially larger) spikes are observed when the

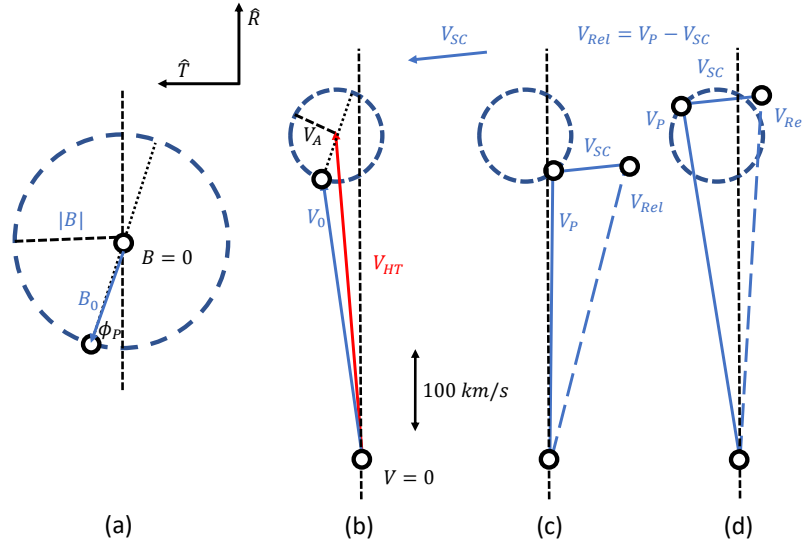


Figure 7. The direction at which the spacecraft passes through the plasma is dependent on the spike deflection vector. (a) The magnetic field vectors lie on a sphere (here, shown in 2D) due to the Alfvénic nature of the fluctuations; $B = 0$ is at the centre of this sphere and in the absence of fluctuations, B_0 lies at the Parker angle ϕ_P to the radial. (b) Velocity vectors also lie on a sphere of radius V_A , but its centre (in RTN) is at V_{HT} . Near perihelion, V_{HT} has a +T component of ≈ 30 km/s. (c) If a spike deflects in -T, the velocity in RTN becomes nearly radial, but due to the spacecraft velocity of ≈ 90 km/s in +T, the relative velocity V_{Rel} has a significant -T component and has a large angle to radial. (d) If the deflection is in +T, the relative velocity V_{Rel} can become nearly radial. This diagram is approximately to scale for spikes on 2018 day 309.

transverse velocity is small. Here, the transverse velocity relative to V_{HT} , rather than the radial direction, is used. This is physically more meaningful if the structures were aligned with the local background flow, and also shows a slightly better dependence on transverse speed than comparing to the radial or Parker spiral directions, although there is a great deal of statistical scatter. Given how closely aligned are all three directions, it is difficult to distinguish between them statistically.

In an attempt to quantify the size and shape of the spikes, we have calculated the mean spatial extent – the duration of a spike crossing, multiplied by V_{Rel} – as a function of the angle of \mathbf{V}_{Rel} to the underlying flow vector \mathbf{V}_{HT} : this is shown in Figure 8. There is naturally a large error associated with these estimates, both from the angle estimates – probably only accurate to a few degrees at best given that we are using a mean velocity during each spike, and \mathbf{V}_{HT} rather than the true background flow direction – and the duration, since we judge the duration of a spike simply from the time the field deflection passes 30° to the Parker spiral, to when it returns below that value. In particular, any substructure on a spike would naturally be identified as multiple spikes and indeed the distribution of spike durations appears to be a power law (Dudok de Wit et al. 2019) and does not have a peak at any particular scale. Rather, then, we are estimating the relative scale in each direction.

Despite all these uncertainties, there is an apparent angular dependence of the spike size seen in Figure 8, with larger values at smaller angles. The dashed line is not a fit to the data, but the expected functional form for an infinite tube aligned along the background flow (e.g. Archer et al. 2005), $\lambda(\theta) = \lambda_0 / \cos(\theta)$. Here, the transverse scale $\lambda_0 \approx 7 \times 10^3$ km. Clearly the spikes are not infinitely long tubes, but it is challenging to identify a scale for their long axis, given the uncertainties in angles. It seems likely, however, that their long axis is several times that of their transverse scale, at several tens of thousands of km.

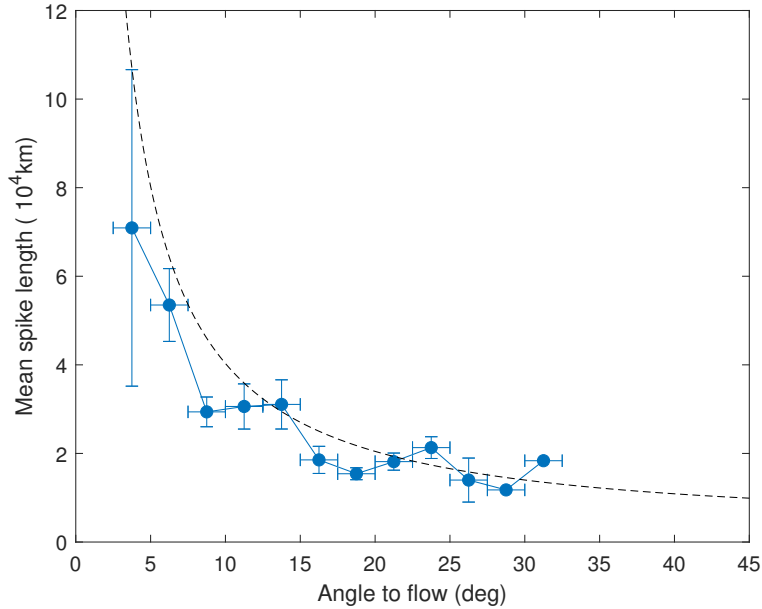


Figure 8. Mean size (in km) of spikes in the two days around perihelion in encounter 1, as a function of the angle at which the spacecraft passed through the spike with respect to the background flow V_{HT} . The dotted line corresponds to an infinite tube with a diameter of 7×10^3 km.

3.2. Comparison with other streams and distances

The question naturally arises whether the spikes at perihelion are typical of those at $35 R_S$ or coronal hole flows in general and indeed whether they are similar structures to those in Helios data. Fortuitously, PSP passed through a more conventional high speed coronal hole stream after perihelion: here, we consider the four days 2018 322-325 (November 18-21) inclusive, when the spacecraft travelled between 83 and 99 R_S . The solar wind speed was between 400 and 600 km/s and $V_A \approx 70$ km/s. Spikes were present throughout, with some quieter gaps lasting several hours which are reminiscent of those in the Helios stream studied by Horbury et al. (2018), but the “patch” variation seen at $35 R_S$, with long term modulations of the spike amplitudes, was not present.

The high wind speed and slow spacecraft motion of around 40 km/s in the +T direction during the stream meant that the spacecraft passed through spikes at only a relatively narrow range of angles compared to the case near perihelion. Applying the method of section 3.1 reveals sizes of $\approx 6 \times 10^4$ km at angles of $\approx 10^\circ$ to the HT frame, consistent with those at perihelion.

We conclude that the spikes seen at perihelion during encounter 1 are likely to be consistent with those previously reported, and those observed elsewhere by PSP, but the complex interplay between spacecraft motion, stream flow speed and spike deflection results in a significantly different character in the time series at these different locations.

4. DISCUSSION

We have presented an early analysis of some aspects of the properties of solar wind velocity spikes in the solar wind near $35 R_S$. These appear to be qualitatively similar to those previously seen at larger distances despite the unusual nature of the source coronal hole resulting in a slow but Alfvénic wind. This low speed, combined with the near co-rotation of the spacecraft at perihelion, resulted in unique observations which make it possible to determine properties of the events which could not otherwise be achieved.

The spikes appear to be elongated, probably along the flow but possibly along the background magnetic field – these two directions are too closely aligned to make a clear distinction – and their transverse scale is of order 10^4 km. They are Alfvénic and contain substantial substructure; some are associated with decreases in the field magnitude, but most are not. Individual spikes tend to deflect in one direction, as arcs, before returning to the original direction. Different spikes deflect in different directions, but groups of spikes sometimes have a consistency of deflection.

It is natural to compare the observed properties of spikes with what might be expected from a coronal jet. Unlike most remote observations of jets (e.g. Dobrzycka et al. 2002) and fine scale structure of the near-Sun solar wind (Raymond et al. 2014; DeForest et al. 2016) – and indeed some previous observations of fine scale solar wind substructure (Borovsky 2008) – the events observed here do not have large density contrast, in common with those seen in Helios (Horbury et al. 2018). If the spikes are indeed related to coronal jets, it might be that the plasma jet is assimilated into the ambient plasma, leaving only the Alfvénic fluctuations to propagate into the solar wind (Roberts et al. 2018), or that the plasma in the jet is not sufficiently energetic to escape the Sun’s gravity.

The spikes at perihelion of PSP’s first orbit tend to occur in “patches” lasting several hours, separated by much quieter intervals. The duration of these patches might be the result of the Parker Solar Probe orbit. The first three orbits of Parker Solar Probe are unique in that the spacecraft tangential velocity near perihelion, around 90 km/s, was close to the corotation velocity at the spacecraft distance. This, combined with the large expansion factor of the flow from the small equatorial coronal hole in which it originated, means that the footpoint motion of the spacecraft was lower than has ever been achieved by a spacecraft before. Ballistic projection to $2.5 R_S$ followed by a Potential Field Source Surface mapping based on GONG magnetograms (see also Badman et al. 2019) suggests that the spacecraft magnetic footpoint moved at around 100 km/hour during perihelion. While such numbers have, by their very nature, large uncertainties, if particular regions within the equatorial coronal hole were generating jets, for example coronal bright points or lanes between supergranules, the duration of the patches at PSP could correspond to the spatial scale of these regions rather than the duration of activity of a given region. Indeed, given a duration of several hours, individual patches seem unlikely to be the result of a single coronal jet, but rather could represent a region within a coronal hole flow – for example a plume – below which multiple jets occur. PSP measurements of a coronal hole at larger distances did not exhibit the same patchy modulation of spike amplitudes. A similar analysis of the footpoint motion of the spacecraft for that stream resulted in values of up to $\approx 10^3$ km/hour, an order of magnitude higher than at perihelion. If the duration of patches of spikes at PSP during perihelion, of several hours, was due to the slow tracking of the spacecraft over source regions, the corresponding timescale during this later stream would be less than an hour. This timescale is only a few multiples of the time between spikes seen at perihelion, so it might be that the quiet, inter-patch intervals seen at perihelion cannot be identified at larger distances and would not ever be seen at other spacecraft.

The preference for the magnetic field to deflect in particular directions within spikes, and the consistency of this direction within patches, is hard to explain. One possible cause might be large scale, non-radial magnetic field components in the lower corona, causing preferential interchange reconnection in a given direction and hence a preferred sense of deflection of the resulting Alfvénic spike.

Using our crude spike identification algorithm, 46% of the coronal hole flow was filled with spikes, but patches filled perhaps three quarters of the perihelion stream. This is a significant challenge to theories of their origin: remote observations of conventional coronal jets do not come close to this frequency, although jetlets (Raouafi & Stenborg 2014) seem more common. While smaller events, below the resolution of existing telescopes, might well be more numerous, and simulations of jets suggest that individual events shred into elongated complex structures which could result in multiple apparent spikes at a spacecraft, the near-ubiquity of the spikes is notable.

Some other spike properties are more consistent with remote observations of jets and waves, with durations of seconds to minutes and speeds of ≈ 100 km/s above the background wind. Transverse scales of 10^4 km are also similar to some observations (e.g. Raouafi et al. 2016) but perhaps surprising: given the overexpansion of the flow from the equatorial coronal hole, combined with a transverse expansion due to conserving a solid angle extent, one might expect the cross-flow scale at $35 R_S$ to be much larger than that near the Sun. Again, though, since the complex outflow from one single near-Sun event could result in many spikes at PSP, it is hard to make a quantitative comparison between these two scales.

Many spikes have magnetic field deflections of more than 90° - this is a well known property of low frequency fluctuations in the solar wind, where $\delta \mathbf{B}/B \approx 1$ (Bruno & Carbone 2013). It is, however, challenging to models of the formation of such structures; recent simulations (e.g. Roberts et al. 2018; Wyper et al. 2017) do not generate such large deflections. Indeed, the configuration of the magnetic field within these events is not clear at this time (Tenerani 2019) and will require considerable future work. Nevertheless, the observations of propagating Alfvénic fluctuations away from coronal jets (Nistico et al. 2010) are broadly consistent with what is observed at PSP.

Perhaps the most notable characteristics of the spikes that suggest a jet origin are their bursty, intermittent nature; their organisation into patches; and their non-random sense of magnetic field deflection in time. All of these seem

qualitatively consistent with a jet origin, but are far harder to explain from simple coronal waves. Nevertheless, the origin of the spikes, and their ultimate role in the generation and acceleration of the solar wind, remains unclear for now. In the near future, PSP perihelia far closer to the Sun, particularly combined with simultaneous remote sensing data, are likely to resolve these issues.

5. ACKNOWLEDGMENTS

We are grateful to David Stansby and Denise Perrone for useful conversations. Tim Horbury was supported by STFC grant ST/S000364/1, Thomas Woolley by ST/N504336/1 and Ronan Laker by an Imperial College President's scholarship. Stuart Bale acknowledges support from the Leverhulme Trust. M Velli was supported by the PSP OS grant NNX 15AF34G. Ben Chandran was supported by NASA grants NNX17AI18G and 80NSSC19K0829. This work made use of the open-source and free community-developed space physics, potential field modelling, trajectory and solar data analysis packages HeliPy (Stansby et al. 2019); pfsspy (Stansby 2019); SpiceyPy (Annex et al. 2019); and Sunpy (SunPy Community et al. 2015).

REFERENCES

- Annex, A., Carcich, B., kd7uui, et al. 2019, AndrewAnnex/SpiceyPy: SpiceyPy 2.3.1, v2.3.1, Zenodo, doi: [10.5281/zenodo.3509530](https://doi.org/10.5281/zenodo.3509530)
- Archer, M., Horbury, T. S., Lucek, E. A., et al. 2005, *Journal of Geophysical Research-Space Physics*, 110, doi: [ArtnA0520810.1029/2004ja010791](https://doi.org/10.1029/2004ja010791)
- Badman, S. T., Bale, S. D., Oliveros, J. C. M., et al. 2019, *The Astrophysical Journal Supplement (ApJS)*, in press
- Bale, S. D., Goetz, K., Harvey, P. R., et al. 2016, *Space Science Reviews*, 204, 49, doi: [10.1007/s11214-016-0244-5](https://doi.org/10.1007/s11214-016-0244-5)
- Bale, S. D. e. a. 2019, *Nature*, in press
- Borovsky, J. E. 2008, *Journal of Geophysical Research-Space Physics*, 113, 25, doi: [10.1029/2007ja012684](https://doi.org/10.1029/2007ja012684)
- Bruno, R., & Carbone, V. 2013, *Living Reviews in Solar Physics*, 10, 7, doi: [10.12942/lrsp-2013-2](https://doi.org/10.12942/lrsp-2013-2)
- Certain, J. W., Golub, L., Lundquist, L., et al. 2007, *Science*, 318, 1580, doi: [10.1126/science.1147050](https://doi.org/10.1126/science.1147050)
- Cranmer, S. R. 2002, *Space Science Reviews*, 101, 229, doi: [Doi10.1023/A:1020840004535](https://doi.org/10.1023/A:1020840004535)
- Culhane, L., Harra, L., Baker, D., et al. 2007, *Publications of the Astronomical Society of Japan*, 59, S751, doi: [10.1093/pasj/59.sp3.S751](https://doi.org/10.1093/pasj/59.sp3.S751)
- De Pontieu, B., McIntosh, S. W., Carlsson, M., et al. 2007, *Science*, 318, 1574, doi: [10.1126/science.1151747](https://doi.org/10.1126/science.1151747)
- DeForest, C. E., Matthaeus, W. H., Viall, N. M., & Cranmer, S. R. 2016, *Astrophysical Journal*, 828, doi: [Artn6610.3847/0004-637x/828/2/66](https://doi.org/10.1086/6610.3847/0004-637x/828/2/66)
- Dobrzycka, D., Cranmer, S., Raymond, J., Biesecker, D., & Gurman, J. 2002, *Astrophysical Journal*, 565, 621, doi: [10.1086/324431](https://doi.org/10.1086/324431)
- Dudok de Wit, T., Krasnoselskikh, V. V., Bale, S. D., et al. 2019, *The Astrophysical Journal*, submitted
- Fox, N., Velli, M., Bale, S., et al. 2016, *Space Science Reviews*, 204, 7, doi: [10.1007/s11214-015-0211-6](https://doi.org/10.1007/s11214-015-0211-6)
- Gosling, J. T., Tian, H., & Phan, T. D. 2011, *Astrophysical Journal Letters*, 737, doi: [ArtnL3510.1088/2041-8205/737/2/L35](https://doi.org/10.1088/2041-8205/737/2/L35)
- Hapgood, M. A. 1992, *Planetary and Space Science*, 40, 711, doi: [10.1016/0032-0633\(92\)90012-d](https://doi.org/10.1016/0032-0633(92)90012-d)
- Horbury, T. S., Matteini, L., & Stansby, D. 2018, *Monthly Notices of the Royal Astronomical Society*, 478, 1980, doi: [10.1093/mnras/sty953](https://doi.org/10.1093/mnras/sty953)
- Kasper, J. C., Abiad, R., Austin, G., et al. 2016, *Space Science Reviews*, 204, 131, doi: [10.1007/s11214-015-0206-3](https://doi.org/10.1007/s11214-015-0206-3)
- Kasper, J. C. e. a. 2019, *Nature*, in press
- Khrabrov, A., & Sonnerup, B. 1998, *ISSI Scientific Reports Series*
- Matteini, L., Horbury, T. S., Neugebauer, M., & Goldstein, B. E. 2014, *Geophysical Research Letters*, 41, 259, doi: [10.1002/2013gl058482](https://doi.org/10.1002/2013gl058482)
- Matteini, L., Horbury, T. S., Pantellini, F., Velli, M., & Schwartz, S. J. 2015, *Astrophysical Journal*, 802, doi: [Artn1110.1088/0004-637x/802/1/11](https://doi.org/10.1088/0004-637x/802/1/11)
- Neugebauer, M. 2012, *Astrophysical Journal*, 750, doi: [Artn5010.1088/0004-637x/750/1/50](https://doi.org/10.1088/0004-637x/750/1/50)
- Nistico, G., Bothmer, V., Patsourakos, S., & Zimbardo, G. 2010, *Annales Geophysicae*, 28, 687, doi: [10.5194/angeo-28-687-2010](https://doi.org/10.5194/angeo-28-687-2010)
- Patsourakos, S., Pariat, E., Vourlidis, A., Antiochos, S. K., & Wuelser, J. P. 2008, *ApJL*, 680, L73, doi: [10.1086/589769](https://doi.org/10.1086/589769)
- Phan, T. 2019, *Ap. J.*, submitted
- Raouafi, N. E., Petrie, G. J. D., Norton, A. A., Henney, C. J., & Solanki, S. K. 2008, *ApJL*, 682, L137, doi: [10.1086/591125](https://doi.org/10.1086/591125)

- Raouafi, N. E., & Stenborg, G. 2014, *ApJ*, 787, 118, doi: [10.1088/0004-637X/787/2/118](https://doi.org/10.1088/0004-637X/787/2/118)
- Raouafi, N. E., Patsourakos, S., Pariat, E., et al. 2016, *Space Science Reviews*, 201, 1, doi: [10.1007/s11214-016-0260-5](https://doi.org/10.1007/s11214-016-0260-5)
- Raymond, J. C., McCauley, P. I., Cranmer, S. R., & Downs, C. 2014, *Astrophysical Journal*, 788, doi: [Artn15210.1088/0004-637x/788/2/152](https://doi.org/10.1088/0004-637x/788/2/152)
- Roberts, M. A., Uritsky, V. M., DeVore, C. R., & Karpen, J. T. 2018, *Astrophysical Journal*, 866, 18, doi: [10.3847/1538-4357/aadb41](https://doi.org/10.3847/1538-4357/aadb41)
- Stansby, D. 2019, *dstansby/pfsspy: pfsspy 0.1.2, 0.1.2*, Zenodo, doi: [10.5281/zenodo.2566462](https://doi.org/10.5281/zenodo.2566462)
- Stansby, D., Rai, Y., JeffreyBroll, et al. 2019, *heliopython/heliopy: HelioPy 0.8.1, 0.8.1*, Zenodo, doi: [10.5281/zenodo.3368264](https://doi.org/10.5281/zenodo.3368264)
- SunPy Community, T., Mumford, S. J., Christe, S., et al. 2015, *Computational Science and Discovery*, 8, 014009, doi: [10.1088/1749-4699/8/1/014009](https://doi.org/10.1088/1749-4699/8/1/014009)
- Tenerani, A. 2019, *Ap. J.*, submitted
- Thieme, K. M., Marsch, E., & Schwenn, R. 1990, *Annales Geophysicae-Atmospheres Hydrospheres and Space Sciences*, 8, 713. [⟨GotoISI⟩://WOS:A1990EH72100001](https://www.ingenta.com/doi/10.1007/BF02431111)
- Tian, H., DeLuca, E. E., Cranmer, S. R., et al. 2014, *Science*, 346, 4, doi: [10.1126/science.1255711](https://doi.org/10.1126/science.1255711)
- Uritsky, V. M., Roberts, M. A., DeVore, C. R., & Karpen, J. T. 2017, *Astrophysical Journal*, 837, doi: [ARTN12310.3847/1538-4357/aa5cb9](https://doi.org/10.3847/1538-4357/aa5cb9)
- Wang, Y. M., Sheeley, N. R., J., Socker, D. G., et al. 1998, *ApJ*, 508, 899, doi: [10.1086/306450](https://doi.org/10.1086/306450)
- Whittlesey, P. 2019, *Ap. J.*, submitted
- Wyper, P. F., Antiochos, S. K., & DeVore, C. R. 2017, *Nature*, 544, 452, doi: [10.1038/nature22050](https://doi.org/10.1038/nature22050)
- Yu, H. S., Jackson, B. V., Buffington, A., et al. 2014, *ApJ*, 784, 166, doi: [10.1088/0004-637X/784/2/166](https://doi.org/10.1088/0004-637X/784/2/166)